Astron. Astrophys. 116, 80–88 (1982)

ASTRONOMY AND ASTROPHYSICS

The Far-UV Spectrum of the Low-excitation Planetary Nebula HD 138403*

J. Surdej[1,**], and A. Heck[2,***]

[1] Institut d'Astrophysique, Université de Liège, Avenue de Cointe 5, B-4200 Cointe-Ougrée, Belgium
[2] Astronomy Division, ESTEC, European Space Agency, Noordwijk, The Netherlands

Received May 18, accepted June 11, 1982

Summary. The IUE satellite was used to record the first high resolution ($\lambda/\Delta\lambda \sim 1.2\,10^4$) far-ultraviolet spectra ($\lambda\lambda \sim 1170$–2070 Å) of the low-excitation planetary nebula HD 138403.

The most prominent spectral features of this object consist of a stellar continuum cut by numerous interstellar lines, on which are superimposed various types (I, VIII, IX) of P Cygni profiles. Those due to the resonance doublets of N v, C iv, Si iv, etc. and to the He ii λ 1640 line transition indicate the presence of an important mass-loss from the central object, with terminal velocities of the order of 800 km s^{-1}.

The only nebular emissions identified in the far-UV spectrum are the C iii] λ 1909 intercombination line with its associated $2s^{21}\,S_0 - 2s2p^3P_2^0$ magnetic quadrupole transition. Using the ratio of the line fluxes measured for these components, we have derived a value $n_e = 1.1(\pm 0.4)\ 10^5\,\mathrm{cm}^{-3}$ for the electron density in the main nebula.

Furthermore, a remarkable asymmetry in the red wing of the C iii] λ 1908.734 emission profile is found to be consistent with the presence of an emission satellite, shifted by $+123$ km s^{-1} with respect to the central main component. These data support the hypothesis that a bipolar structure is expanding around HD 138403, via the selective radiative process of edge and/or line locking mechanism(s).

Key words: ultraviolet spectra – planetary nebula – HD 138403 – mass-loss

1. Introduction

It is well established (Heap, 1977a, b) that HD 138403 ≡ 315–13°1 ≡ He2–131 is a young, very bright and compact evolving low-excitation planetary nebula whose central nucleus, classified 07(f)eq with a visual absolute magnitude $M_v = -2.1$, undergoes a continuous mass-loss.

Thackeray (1950) has measured a circular disk, about 6″ in diameter, around the central star HD 138403 and Koelbloed (1962) has derived the physical conditions prevailing in the nebula: $n_e = 210^4\,\mathrm{cm}^{-3}$, $T_e = 9000 \pm 1000$ K.

Various observers (cf. Méndez and Niemela, 1979) have reported spectral variations over time scales ranging from a few days to a few tens of years, in the strength and P Cygni profile of various line transitions of He, C, N, and Si ions. Surdej et al. (1982, referred to below as Paper I) have further discussed the variability of the visible spectrum of HD 138403 and they have reported the discovery of faint blue and red satellites, shifted by approximately 124 km s^{-1}, on each side of the Balmer and [O ii] emission lines. Invoking the near coincidence ($v_s = 122$ km s^{-1}) between the wavelengths of line transitions due to $H(n = 1, 2, \ldots \rightarrow n')$ and He ii $(n = 2, 4, \ldots \rightarrow 2n')$, they have interpreted these spectral features in terms of the formation of a bipolar structure, nearly aligned along the line of sight, and driven away from the central star by the selective radiative processes of edge and/or line locking (Milne, 1926).

These conclusions prompted us to obtain ultraviolet observations of this interesting planetary nebula. Two UV spectra have been recorded on last December 1980 at high dispersion with the SWP camera of the IUE satellite (for detailed information about the IUE Satellite instrumentation see Boggess et al., 1978a). These observations are presented and discussed in the next sections. Let us mention that the only far-ultraviolet observations reported so far for HD 138403 have been made using the ANS satellite, in five intermediate bands about 150 Å wide (Pottasch et al., 1978). With this same instrument, Gilra et al. (1978) have detected spectral variations of the C iv resonance doublet at λ 1550 Å, on time scales of half a year.

2. Observations

Two high resolution ($\lambda/\Delta\lambda \sim 1.2\,10^4$) spectra of HD 138403 were obtained on 21 December, 1980 with the International Ultraviolet Explorer (IUE) at the ESA satellite tracking station at Villafranca, Spain (VILSPA). These two echelle spectra cover the same spectral range (~ 1170–2070 Å) in the far-ultraviolet, with a velocity resolution of 25 km s^{-1}. The first spectrum (image SWP 10854), recorded during 180 min, is somewhat underexposed; therefore a second one (image SWP 10855) was taken during the last 200 min of our shift: this spectrum is fairly well exposed longward of λ 1300 Å. Let us directly mention that due to the absence of strong nebular emissions in the ultraviolet spectrum of HD 138403, no line was found to be saturated.

Because the nebula surrounding HD 138403 has an angular size of approximately 6″ and that the IUE large rectangular (10×20″) aperture was used, the recorded spectra are those of the

Send offprint requests to: J. Surdej.

* Based on observations by the International Ultraviolet Explorer collected at the Villafranca Satellite Tracking Station of the European Space Agency

** Chercheur Qualifié au Fonds National de la Recherche Scientifique (Belgium)

*** Permanent address: ESA Satellite Tracking Station, Apartado 54065, Madrid, Spain

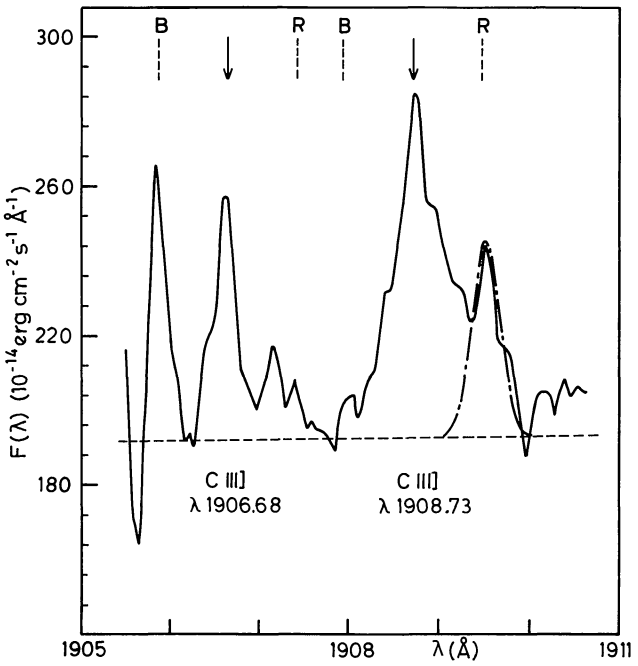

Fig. 1. The C III] line profiles resulting from the average of the two SWP 10854 and SWP 10855 images. The arrows indicate the rest positions of the two C III] components at $\lambda\lambda$ 1906.68 and 1908.73 Å. The dashed vertical bars correspond to the hypothetical positions of the red and blue emission satellites associated with these central components. The dot-dashed line represents a gaussian profile fitted to the λ 1908.73 red emission satellite (see text). The adopted continuum level is shown by the horizontal dashed line

whole planetary nebula with its central star. These spectra were processed at VILSPA with the standard routines (see Boggess et al., 1978b and the subsequent NASA and ESA IUE Newsletters).

3. The Far-ultraviolet Spectrum

As a whole, the far-ultraviolet spectrum of HD 138403 may be characterized by a stellar continuum on which are superimposed a few emission lines (see Sect. 3.1) and a great variety of different types of P Cygni profiles (see Sect. 3.2). The spectrum is also marked by the presence of many interstellar absorptions (see Sect. 3.3).

The identification of line transitions was made on the basis of the two recorded spectra. Although the signal to noise ratio is generally better on the SWP 10855 image, only those lines appearing on both spectra were considered as definitely present. However, due to the difficulty for defining the continuum in certain spectral regions, for ascertaining the type (emission?, absorption?) of some complex profiles, etc. there remains a non-negligible fraction of unidentified spectral features. The most conspicuous of these are listed in a separate Table (see Sect. 3.4).

We detail and discuss here below each of the principal constituents of the far-UV spectrum of HD 138403.

3.1. Emission Lines

At the short-wavelength end, the strong emission due to Ly α is mostly, if not all, attributable to the geocoronal Ly α emission which fills in the $10 \times 20''$ entrance aperture. As usually, this emission is superimposed on a very shallow absorption due to the interstellar Ly α line.

With the possible exception of the faint emission lines at $\lambda\lambda$ 1304.86, 1306.03 Å due to O I multiplet No. 2 (see Fig. 5, the third line of this multiplet at λ 1302.17 Å being masked by a camera reseau mark located at the same position), the only *nebular* emission identified in the far-UV spectrum of HD 138403 is due to the C III] λ 1908.734 intercombination line with its associated $2s^2\,{}^1S_0 - 2s2p\,{}^3P_2^0$ magnetic quadrupole transition at λ 1906.68 Å. This constitutes one more rare example of a magnetic quadrupole transition detected in the spectrum of an astronomical object.

The wavelength scales assigned to IUE spectra are derived from Pt-Ne lamp spectra taken at more or less regular intervals. The resulting zero-point uncertainties can be as great as 20–30 km s^{-1} (Harvel, 1980).

In order to find the shift in the wavelength calibration of the large aperture images, we assume that the emission peaks of the C III] lines at $\lambda\lambda$ 1907, 1909 Å originate in a frame at rest with respect to the central star. Out of 33 nebular emissions in the visible spectrum, the heliocentric radial velocity of HD 138403 was determined to be $v = 7 \pm 3$ km s^{-1} (see Paper I). We therefore shifted in wavelength the IUE spectra in order to achieve the desired consistency in the heliocentric radial velocity of the nebula surrounding HD 138403.

We have illustrated in Fig. 1 the C III] line profiles as the result of averaging the two image spectra. The arrows which are drawn in that figure indicate the rest positions of the two C III] components at $\lambda\lambda$ 1906.68 and 1908.734 Å.

It is then remarkable to see on that tracing the presence of a strong asymmetry in the red wing of the C III] λ 1908.734 emission. Of course, this feature is similarly well displayed on both individual spectra. Since the velocity separation between this spectral feature and the main central component amounts to $+123 \pm 13$ km s^{-1} and since the presence of emission satellites, red- and blue-shifted by about 122 km s^{-1}, is well established for the Balmer ($H_\beta - H_9$) and [O II] $\lambda\lambda$ 3726, 3729 lines (see Sect. 1 and Paper I for further details), it is straightforward to identify the above feature with the red emission satellite due to the C III] dipole transition.

The dashed vertical bars represented in Fig. 1 correspond to the hypothetical positions of those red and blue emission satellites shifted by 122 km s^{-1} with respect to their central components. The probable absence of the blue (resp. red) emission satellite associated with the dipole (resp. magnetic quadrupole) transition of C III] is striking but it may be simply interpreted as being caused by large differences between the emissivity, electron density, etc. prevailing in the two lobes of the bipolar structure from which, we assume (see Paper I), they arise. Despite the near coincidence between the emission feature seen at λ 1905.9 Å and the hypothetical position of the blue satellite associated with the magnetic quadrupole transition of C III], we cannot ascertain the reality of this observation due to the poor photometric accuracy existing at the extreme edge of spectral order No. 72. Therefore, the presence of this blue satellite remains questionable and should be confirmed on better quality data.

For the case of a homogeneous optically thin gaseous nebula, Osterbrock (1970) has first mentioned the possibility of determining electron densities from the observed intensity ratio of the two C III] components. The very small sensitivity of this ratio to temperature is well illustrated by the theoretical dependence of the

Table 1. Electron densities derived from the ratio of the two $^1S_0 - {}^3P^0_{1,2}$ components of C III] associated with the main and satellite emissions (see Nussbaumer and Schild, 1979)

Line flux x 10^{14} (erg $cm^{-2}s^{-1}$)	Main Component	Red Satellite	Blue Satellite
Dipole transition (λ 1908.73)	58.1 $\pm$12.7	20.2*	< 1.3 $\pm$0.3
Magnetic quadrupole transition (λ 1906.68)	19.1 $\pm$1.0	< 2.5 $\pm$0.9	?
Electron density $n_e(cm^{-3})$	1.1($\pm$0.4) 10^5	> 3.7 10^5	-

* Line flux of the theoretical gaussian profile (see text and Fig. 1)
? Uncertain photometric accuracy (see text)

emissivity ratio $\varrho(\lambda 1906.68/\lambda 1908.73)$ as a function of the electron density and temperature (see Loulergue and Nussbaumer, 1976[1]; Nussbaumer and Schild, 1979).

Under the hypothesis that the red satellite associated with the dipole transition of C III] has a gaussian profile (see the dot-dashed line in Fig. 1) with a FWHM = 57.4 km s^{-1}, we have measured the effective line flux of the central component as well as that of the other central component and satellites. The mean values of these line fluxes, based upon measurements of both IUE spectra, are summarized in Table 1. By means of the theoretical values of ϱ, versus n_e and T_e, given in Nussbaumer and Schild (1979), we have also indicated in Table 1 the resulting electron densities, assuming an electron temperature $T_e = 10{,}000$ K (Koelbloed, 1962).

The value $n_e = 1.1(\pm 0.4)\,10^5$ cm^{-3} (see Table 1), inferred for the electron density in the main nebula, appears somewhat larger than the one $n_e = 210^4$ cm^{-3} derived by Koelbloed (1962) on the basis of the ratio $\varrho(\lambda 3729/\lambda 3726)$ observed for the [O II] doublet[2]. However, within the uncertainties affecting our electron density determination and those inherent to the equivalent width measurements of strong forbidden lines on photographic emulsions (Koelbloed, 1962), the agreement between these two independent results is not so bad.

As to the value derived for the electron density in the receding lobe ($v_s = +122$ km s^{-1}) of the bipolar structure, we can only state that it is at least three times greater than the density prevailing in the main nebula (see Table 1).

3.2. P Cygni-*type Profiles*

Evidence for mass-loss from the central star of the planetary nebula 315–13°1 is well established from the analysis of its visual spectrum: P Cygni-like profiles are seen for various line transitions of He, C, N, and Si ions. A typical value for the velocity separation between the emission peak and the most blueshifted edge of the P Cygni absorption is $\overline{v_{ea}} = -127 \pm 38$ km s^{-1} (Thackeray, 1956). Despite the similarity between the values of $\overline{v_{ea}}$ and v_s, it was concluded in Paper I that the mass-loss mechanism leading to the formation of the observed P Cygni profiles was essentially different from that responsible for the presence of the emission satellites.

Therefore, when discovering for the first time the far-UV spectrum of HD 138403 on the console screen of the data acquisition system of VILSPA, we were not surprised to see velocity shifts greater than 500 km s^{-1} in the well developed C IV and Si IV P Cygni profiles (see Figs. 2 and 3). A detailed analysis of the IUE spectra has further revealed that there was a great number of other P Cygni profiles (see Figs. 4–7) associated with line transitions of both low- and high-ion stages.

Following Beals (1951) who has classified eight different types of P Cygni profiles, we shall retain the following ones:

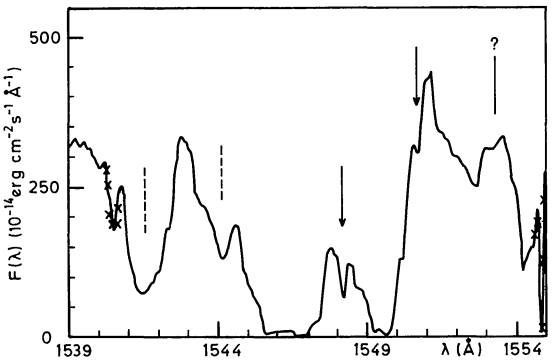

Fig. 2. The C IV resonance doublet P Cygni profiles (smoothing of SWP 10855 spectrum). The arrows indicate the rest positions of the two C IV components at $\lambda\lambda$ 1548.185, 1550.774 Å. The dashed vertical bars correspond to the hypothetical positions of C IV absorptions blue-shifted by 1288 km s^{-1} (see text). In this and all subsequent figures, crosses refer to the presence of camera reseau marks and an interrogation mark denotes an unidentified spectral feature

1 logϱ should be replaced by ϱ in Fig. 4 of that paper
2 As noted by the referee, this ratio can hardly point to values $n_e > 2\,10^4$ cm^{-3} because of saturation

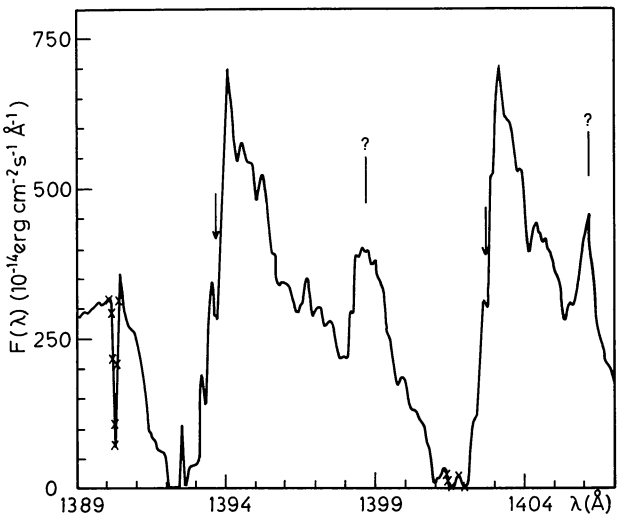

Fig. 3. The Si IV resonance doublet P Cygni profiles (smoothing of SWP 10855 spectrum). The arrows indicate the rest positions of the two Si IV components at $\lambda\lambda$ 1393.755, 1402.770 Å

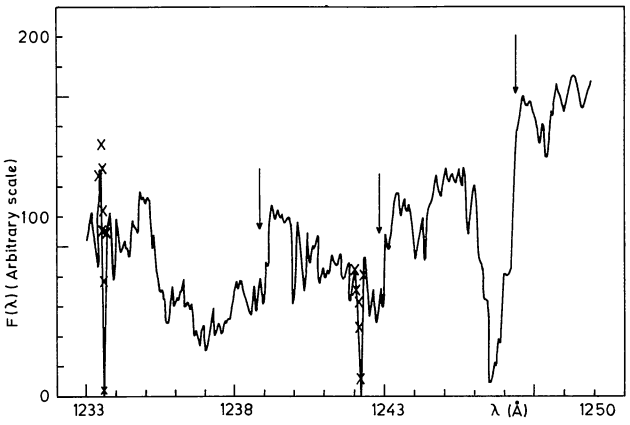

Fig. 4. Type VIII P Cygni profiles for the N V resonance doublet and the C III λ 1247.382 line transition (smoothing of SWP 10855 spectrum). The arrows indicate the rest positions of the two N V components at $\lambda\lambda$ 1238.821, 1242.804 Å and that of C III λ 1247.382. The flux scale is arbitrary (uncertain calibration below λ 1250 Å)

type I: the emission is near its laboratory wavelength in the star's frame and there is an accompanying blueshifted absorption,

type VIII: as type I but the emission component is absent.

We shall also consider an additional type IX (cf. Snow and Morton, 1976) consisting of an asymmetric line with an unshifted minimum and an extended wing on the short-wavelength side.

With that classification, we have reported in Table 2 the identification and type of all observed P Cygni profiles, together with the velocities (relative to the star) of the short-wavelength edge, of the line center of the absorption component and of the peak at half maximum of the emission, if present. Whenever relevant, additional remarks appear at the end of that Table.

A short look at Table 2 leads us to conclude that lines showing type I, VIII or IX P Cygni profiles have been found in the far-UV spectrum of HD 138403 for C II, III, IV; N III, IV, V; O IV, V; Si III, IV; and He II, giving this object the largest variety of ions so far observed in the wind of a nucleus of planetary nebula.

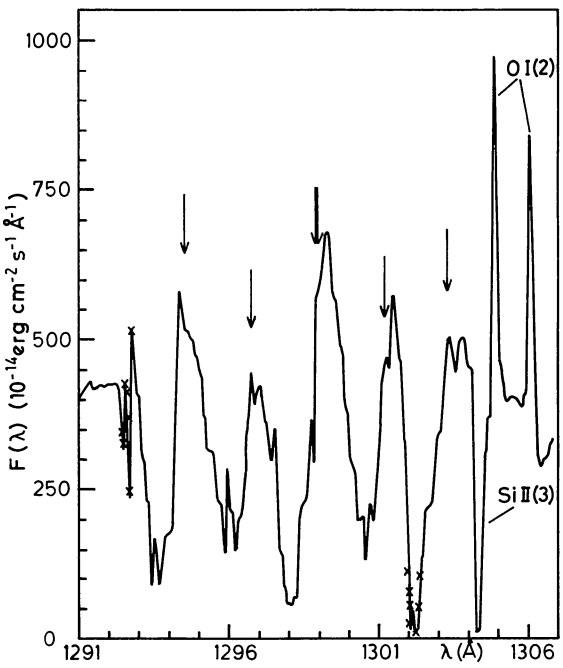

Fig. 5. P Cygni profiles for the Si III (4) line transitions (smoothing of SWP 10855 spectrum). The arrows indicate the rest positions of the six Si III (4) components (see Table 2). Also indicated are the emission lines at $\lambda\lambda$ 1304.86, 1306.03 Å due to O I (2) and the Si II λ 1304.372 interstellar absorption

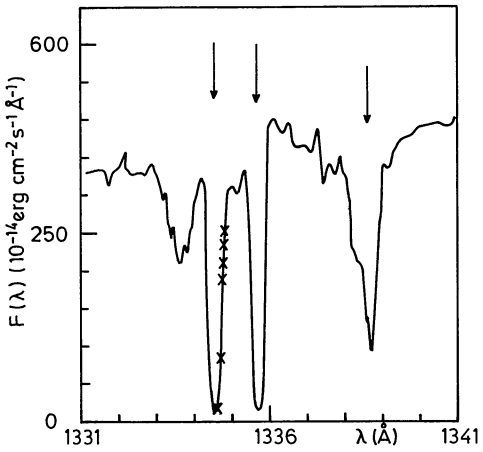

Fig. 6. Type VIII and IX P Cygni profiles for the C II λ 1334.532 and O IV λ 1338.612 line transitions, respectively (smoothing of SWP 10855 spectrum). The arrows indicate the rest positions of the C II $\lambda\lambda$ 1334.532, 1335.703 and O IV λ 1338.612 components. The interstellar absorptions due to C II (1) are nearly saturated

Considering only the resonance P Cygni profiles in Table 2, there appears to be a net correlation between the observed edge velocities and the total ionization potentials of the corresponding ions. The trend of this correlation is of course an increase of the maximum observed velocity with the total ionization potential. It is very probable that this relation reflects an increase of the ionization temperature with the height in the wind of the central nucleus (cf. relation 7c in Olson, 1978). Furthermore, on the basis of the striking similarities between the UV spectral characteristics

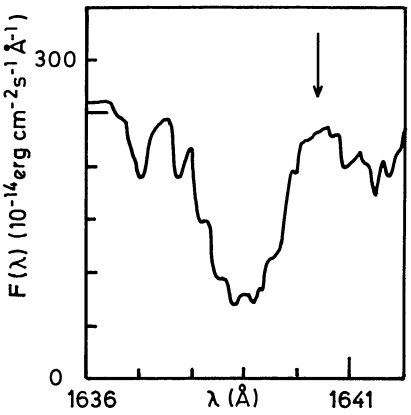

Fig. 7. Type VIII P Cygni profile for the He II (12) line transitions (smoothing of SWP 10855 spectrum). The arrow indicates the rest position of these components at λ 1640.428 Å

of HD 138403 (see remarks in Table 2) and those found in O-type supergiants, it is not excluded that a high temperature corona may be somewhere required in the flow in order to account for the NV blueshifted absorption lines. Observations of the O VI resonance doublet at $\lambda\lambda$ 1031.928, 1037.619 Å in the spectrum of HD 138403 would be a crucial test for this hypothesis. Let us still mention that the edge velocities observed for the subordinate line transitions of a given ion [cf. Si IV $\lambda\lambda$ 4088.863, 4116.104; C II $\lambda\lambda$ 4267.02, 4267.27; etc. in Thackeray (1956) and Si III(4) in Table 2] are found systematically smaller than those associated with the corresponding resonance line transitions [cf. Si IV(1), C II(1), Si III(2) in Table 2]. This effect is well known from spectral studies of various other O-type stars for which a velocity-excitation relation has been firmly established (cf. Hutchings, 1978): as expected on theoretical grounds, the excitation temperatures decrease with increasing distance from the photosphere.

Due to the large uncertainties affecting our determinations of the edge velocity for the N V and C IV resonance doublet profiles,

Table 2. Velocities (km s^{-1}) of the P Cygni profiles in the far-UV spectrum of HD 138403

Line transition (Kelly and Palumbo, 1973)		P Cygni type	Velocities and error estimates* Edge	Center	Em.	Remarks (Explanation below Table)
C III(4)	1174.933 Å 1176.370	I	-438 ±91	-	R	1
Si III(2)	1206.510	VIII?	-551 ±82	R		2
N V(1)	1238.821	VIII	[-657, -822]	-391 ±48		3, see Fig. 4
	1242.804	VIII	[-475, -716]	R		
C III(9)	1247.382	VIII	-293 ±35	-134 ±25		see Fig. 4
Si III(4)	1294.543	I	-336 ±50	-223 ±50	27 ±50	4, see Fig. 5
	1296.726	I-VIII?	-342	-154	—	
	1298.891 1298.960	I	-326	-194	61	
	1301.146	I	-308	-153	61	
	1303.320	I	R	R	—	
C II(1)	1334.532	VIII	-344 ±25	-198 ±25		5, see Fig. 6
O IV	1338.612	IX	-165 ±40	+4 ±10§		6, see Fig. 6
	1342.992 1343.512	IX	-126 —	— —		
O V(7)	1371.292	IX	-287 ±80	-3 ±10§		7
Si IV(1)	1393.755	I	-629 ±35	-271 ±50	199 ±70	8, see Fig. 3
	1402.770		-681 ±70	-276	160	
C IV(1)	1548.185 1550.774	I? I	<-853 ±60? —	— -278 ±45	— 105 ±40	9, see Fig. 2
He II(12)	1640.332 1640.474 1640.490	VIII	-445 ±35	-260 ±35		10, see Fig. 7
N IV(7)	1718.551	VIII	-483 ±45	-292 ±45		
N III(19)	1747.86	VIII	-275 ±45	-47 ±45		11
	1751.24 1751.75	VIII	R	R		

Explanation of symbols

* - The error estimates represent r.m.s. values as derived from three independent measurements of the velocities on both IUE spectra. Because the velocity determinations depend on the accurate setting of the continuum level, on the exact location of the absorption edge, etc. one should be aware that the values reported in Table 2 are somewhat subjective and that the error estimates should be just considered as internal deviations of our velocity determinations.

Edge - Velocity, as measured in the star's frame, of the short-wavelength edge of the P Cygni absorption.

Center - Velocity, as measured in the star's frame, of the center of the absorption component or its minimum, if asymmetric.

Em. - Velocity, as measured in the star's frame, of the peak at half maximum of the emission component.

R - Denotes the presence of a camera reseau mark at the position of the corresponding feature.

? - Stands for uncertain.

§ - The nearly zero velocity observed for the unshifted minimum of these type IX profiles if fully consistent with the zero-point correction applied to the wavelength scale of both IUE spectra (cf. Section 3.1).

} - Denotes a blend between two or more line transitions.

Additional remarks to Table 2

1 Multiplet No. 4 of C III consists of six line transitions in the range λλ 1174.933, 1176.370 Å. The edge velocity was therefore derived on the basis of the λ 1174.933 transition but no center velocity could be inferred. For this six-lines multiplet, Snow and Morton (1976) report the presence of well developped P Cygni profiles in the spectrum of all supergiants, bright giants and giants with spectral types O4-O9, but none are found in the spectrum of dwarfs and subgiants.

2 The wide absorption due to Ly α as well as the presence of an interstellar absorption due to Si III(2) prevent the detection of a possible emission near the rest position. In all supergiants ranging from O7Ia to B0.5Ia, the Si III(2) line profile displays large velocity displacements (Snow and Morton, 1976).

3 The N V resonance doublet profiles are ill-defined but definitely present on both IUE spectra (see Fig. 4). Although the presence of interstellar and/or circumstellar features cannot be totally excluded (cf. Section 3.3), the N V profiles appear to be mainly composed of optically thin, blueshifted absorptions. Let us further mention that P Cygni type profiles are observed for N V in all stars hotter and more luminous than Bo (Abbott, Bohlin and Savage, 1982) and that their presence in hot supergiants probably requires the existence of a high temperature stellar corona (Snow and Morton, 1976)

4 Fig. 5 clearly shows that for all type I P Cygni profiles due to Si III(4), the equivalent width of the emission component is much smaller than that of the shifted absorption. It is also quite possible that there is an overlap between the red wing of the emission component and the short-wavelength edge of the absorption of two consecutive profiles. Due to the presence of a TV reseau mark at λ ∼ 1302 Å and of the Si II λ 1304.372 interstellar feature, no velocities are reported for the Si III(4) λ 1303.320 profile. Let us finally note that for stars with spectral types later than O7, absorption lines coinciding with the line transitions of Si III(4) are evident in the Snow and Jenkins (1977)'s atlas of P Cygni spectra.

5 Additional cases of type VIII P Cygni profiles observed for the C II λλ 1334.5, 1335.7 transitions in the spectrum of early-type stars are reported by Snow and Morton (1976).
The presence of a reseau mark at λ 1335 and of the deep C II(1) λλ 1334.532, 1335.703 interstellar absorptions prevent the detection of a type VIII profile for the C II(1) λ 1335.703 component (see Fig. 6).

6 Similar asymmetric lines are seen for O IV λλ 1338.612-1343.512 in the far-UV spectrum of ζ Puppis, ρ Ori, δ Ori A and ζ Ori A (Snow and Morton, 1976).

7 A similar profile is observed for the line transition O V(7) λ 1371.292 in the spectrum of ζ Puppis (Snow and Morton, 1976).

8 The Si IV resonance doublet P Cygni profile usually provides a good mass-loss indicator in O4-B0.5 supergiants. However, the saturation of the shifted absorptions prevents us to make such an analysis (see text).

9 The C IV resonance doublet profile is rather complex (see Fig. 2). As for the case of the Si IV doublet, the P Cygni absorptions are-nearly ? - saturated. Furthermore, it is very likely that the two absorption features near λ 1541.4 and λ 1544.2 Å are also attributable to C IV in a high velocity cloud with $v_{center} \sim -1288$ km s^{-1}. Indeed, there is a good agreement in both the position and strength (ratio 2:1) of these absorption components. A reseau mark at λ ∼ 1540.5 Å precludes the determination of the terminal velocity of that cloud.

10 The reported velocities were calculated with a mean effective wavelength λ = 1640.428 Å.

11 It is not excluded that Mg I λ 1747.795 also contributes to the N III λ 1747.86 P Cygni absorption.

we can only state that the terminal velocity of the stellar wind around HD 138403 is of the order of 800 km s^{-1}. However, it is not excluded that matter (blobs?) – transparent to most of spectral line radiations – is also present at velocities as high as 1300 km s^{-1} (cf. remark 9 in Table 2).[3]

Finally, we shall invoke arguments against any attempt of determining a mass-loss rate for HD 138403 from the analysis of its ultraviolet resonance profiles (cf. Olson, 1978; Castor and Lamers, 1979; Surdej, 1980). Indeed, the variability detected at low resolution by Gilra et al. (1978) in the strength and profile of the C IV resonance doublet at $\lambda \sim 1550$ Å, on time scales of six months, should first of all be confirmed on the basis of an additional UV spectrum similar to those analysed here. If, as it is the case for the visible spectrum (see Paper I), spectral variations are found to affect considerably the UV line profiles, it would be a direct proof that the mass-loss around HD 138403 takes place erratically (blobs?) and that, consequently, the approximations of spherical geometry, continuous flow, steady state, etc. inherent to all classical theories of line formation are irrelevant for the present case studied. One indication in favour of such an overview is that the absorption trough in the profiles of the strong C IV (see Fig. 2) and Si IV (see Fig. 3) lines is observed to be at – nearly? – zero intensity over a small range of wavelengths. No theory of line formation built upon the approximations mentioned above can account for such a zero residual intensity.

It is therefore very plausible to assume that the envelope expanding around HD 138403 is not spherically symmetric and that material optically thick to line radiation, moving along the line-of-sight with the required velocity, causes the observed zero residual intensity.

Furthermore, one should be aware that the poor photometric accuracy and/or ill-defined character of certain line profiles (cf. N V in Fig. 4), the saturation of some P Cygni absorptions (cf. the case of C IV and Si IV discussed before), the systematic observed redshift of the peak of the emission component for type I profiles (see Table 2), the relative small range of observed velocities ($\lesssim 800$ km s^{-1}), etc. render very doubtful and questionable the applicability of the only practical methods of mass-loss rate determinations based upon Sobolev-type theories. In this context, we must reject the mass-loss rate estimated by Pottasch (cited as a personal communication in Nussbaumer, 1980) of $10^{-10} M_{\odot}$/yr for He 2-131. The large variety of ions and line transitions

3 Similar components have already been found in the spectra of Wolf-Rayet and other O-type stars (e.g. de Boer and Nash, 1982; Fitzpatrick et al., 1982)

Table 3. Heliocentric velocity and equivalent width of interstellar absorption lines in the far-UV spectrum of HD 138403

Line transition (Kelly and Palumbo, 1973)		Heliocentric velocity (km s^{-1}) and error estimates*	Equivalent width (mÅ) and error estimates*	Remarks (Explanation below Table)
S III(1)	1190.170 } Å	2.6	} 382±44	
Si II(5)	1190.416 }	7.4		
Si II(5)	1193.289	-3.4	674±22	1
N I(1)	1199.550	8.6	239±32	
N I(1)	1200.223	1.3	398±22	
N I(1)	1200.710	11.8	310±29	
Si III(2)	1206.510	-0.4	128± 3	2
N V(1)	1238.808	-4.7	227±35	2, 3, see Fig. 4
N V(1)	1242.796	0.2	175±17	2, 3, see Fig. 4
S II(1)	1250.586	6.9	138±51	
S II(1)	1253.812	9.3	226±47	
S II(1)	1259.520	10.7	183± 6	
Si II(4)	1260.421 }	—	} 363±33	
Fe II(9)	1260.542 }	—		
Si II(4)	1264.737	-11.4?	112±41	4
Si II(3)	1304.372	8.4	290± 5	see Fig. 5
C II(1)	1334.532	R	R	see Fig. 6
C II(1)	1335.703	9.2	196±47	see Fig. 6
Si IV(1)	1393.755	0.8	—	2, see Fig. 3
Si IV(1)	1402.770	7.0	—	2, see Fig. 3
Si II(2)	1526.708	R	R	
C IV(1)	1548.188	5.9	—	2, see Fig. 2
C IV(1)	1550.762	8.0	—	2, see Fig. 2
Fe II(8)	1608.456	-1.6?	—	5
Al II(1)	1670.787	R	R	
Si II(1)	1808.012	21.5?	56±31	6
Zn II(1)	2025.512	6.3	} 388± 7	
Mg I(2)	2025.824	15.4		
Zn II(1)	2062.016	13.4	154± 6	

Explanation of symbols

* - The heliocentric velocity measurements refer to positions of the line centers at half depth. The error estimates in Table 3 represent r.m.s. values as derived from three independent measurements of the velocity and equivalent width of interstellar absorptions on both IUE spectra. Unless otherwise stated, the mean deviations affecting the determination of the heliocentric velocities and equivalent widths amount to 13 km s^{-1} and 25 mÅ, respectively.

R - Denotes the presence of a camera reseau mark at the position of the corresponding feature.

? - Stands for uncertain.

} - Denotes a blend between two line transitions.

Additional remarks to Table 3

1 The absorption line is located between two spectral orders and is therefore affected by a higher noise background.

2 The interstellar (circumstellar ?) absorption is superimposed on the P Cygni absorption due to the same line transition (cf. Table 2).

3 The multi-components appearance of the N V interstellar (circumstellar ?) absorptions is very probably due to noise background. This should, however, be checked on better exposed spectra.

4 The profile of this absorption line is somewhat ill-defined and its identification is therefore only tentative. We have searched for the presence of other absorptions arising from an excited fine structure level of Si II but found only little evidence for the detection of the λλ 1197.394, 1309.278 line transitions.

5 On the blue wing of this sharp absorption, the continuum appears to be affected by the presence of another absorption line. It cannot be excluded that the observed spectral feature is entirely due to Fe II λ 1608.456 (type IX P Cygni profile ?).

6 This line is possibly affected by the presence of an unidentified emission feature.

Table 4. List of unidentified spectral features in the far-UV spectrum of HD 138403

Corrected wavelength	Type of profile (see below)	Remarks (Explanation below Table)
1276.9 Å	a, m, b	1
1320.5	a, m	
1321.5	a, m	
1398.7	e, m, b	see Fig. 3
1406.1	e, m	see Fig. 3
1409.2	a, m	
1430.0	a, m, vb	
1448.8	a, m	
1472.2	a, d, b	
1553.4	e, m, b	see Fig. 2
1591.0	a, m, b	
1620.5	a, m, b	
1646.1 } 1647.5 }	a, d, b } e, m, b }	2
1660.4	e, m	
1661.5	a, m, b	3
1663.8	e, m	
1666.1	e, m	
1680.6	a, m, b	
1687.0	a, m, b	
1764.3 } 1765.3 }	a, m, b } e, m }	2
1819.3	a, m, b	
1827.9	e, m } a, m }	2
1852.4	e, m	
1853.9	a, m, b	
1855.6	e, m, b	
1858.5	e, m	4, see Fig. 8
1860.9	e, m	
1862.1	a, m, b	
1863.6	e, m	

Explanation of symbols used in column 2

a : absorption line.

e : emission line.

m : moderate, i.e. the depth of the line center is smaller than half the continuum level.

d : deep, i.e. the depth of the line center is greater than half the continuum level.

b : broad, i.e. the full width of the spectral feature is greater than 200 km s^{-1}, but smaller than 400 km s^{-1}.

vb : very broad, i.e. the full width of the spectral feature is greater than 400 km s^{-1}.

Additional remarks to Table 4

1 Possible blend of interstellar absorptions due to C I λλ 1276.482, 1277.245 and 1277.513.

2 These absorption and emission components probably form a type I P Cygni profile.

3 It is very tempting to identify the emission lines at λλ 1660.4, 1666.1 Å with O III λλ 1660.803, 1666.153. The observed blueshift of the first emission component is possibly caused by the presence of the unidentified absorption at λ 1661.5 Å.

4 Fig. 8 illustrates very well the ill-defined character of some unidentified spectral features. It is possible that the two sets of absorption and emission components at λλ 1853.9, 1855.6 and λλ 1862.1, 1863.6 Å are type I P Cygni profiles due to the resonance lines of Al III at λ 1854.716 and λ 1862.790 Å. If this is the case, the velocity of the short-wavelength edge of the P Cygni absorptions is about equal to −270 ± 56 km s^{-1}.

observed from the wind of HD 138403, the saturation of the C IV and Si IV P Cygni absorptions, etc. definitely point out to higher mass-loss rates from that 07(f)eq star.

3.3. *Interstellar Absorption Lines*

Although it is not our intention to analyze here the contents of the interstellar medium in front of HD 138403, we feel important to report our observations of interstellar absorption lines in the far-UV. Indeed, due to the location of 315–13°1 in the direction of the Sagittarius-Carina major arm (Georgelin et al., 1979) and because of its large distance from the sun (see Paper I, $D = 2.8 \pm 1.0$ kpc), people interested in modeling the line-of-sight distribution of absorbing clouds, in deriving abundances from curve of growth analysis, etc. could combine our data with others in order to probe the interstellar medium in that direction.

We have reported in Table 3 the heliocentric velocity and equivalent width of all identified interstellar absorptions in the far-UV spectrum of HD 138403. Some of the observed lines are illustrated in Figs. 2–6. Our main conclusions follow:

The interstellar species detected include C II, N I, Mg I, Si II, Si III, S II, S III, Zn II and possibly Al II and Fe II.

The only absorptions arising from an excited fine structure level are found for C II λ 1335.703 and probably for Si II λ 1264.737.

Faint absorption features, identified with interstellar absorptions, are definitely (resp. possibly) present for the two line transitions of the N V, C IV (resp. Si IV) resonance doublets.

The mean heliocentric velocity of all (21) measurable interstellar absorptions amounts to 6 ± 5 km s^{-1}.

Because instrumental blemishes near the rest position of the Si IV, C IV, and N V lines in high resolution IUE spectra have been previously noticed (see Savage and de Boer, 1981) and/or because we are not totally sure of the real origin of the observed faint absorptions (interstellar?, circumstellar?), we shall just mention the possibility that these spectral features arise in very hot interstellar gaseous clouds, collisionally ionized ($T \sim 2\,10^5$ K). We actually stress the importance to collect additional observations before accepting this latter interpretation.

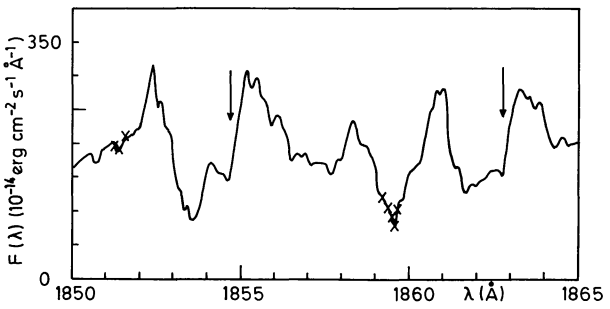

Fig. 8. Example illustrating the ill-defined character of some unidentified spectral features (smoothing of SWP 10855 spectrum). The arrows indicate the rest positions of the resonance lines of Al III λλ 1854.716, 1862.790 (see Table 4)

3.4. *Unidentified Spectral Features*

For the sake of completeness, we present in Table 4 the list of the most conspicuous spectral features which remain unidentified in the far-UV spectrum of HD 138403. The wavelength – corrected for the heliocentric radial velocity of the star – of each spectral feature is given in that Table as well as the type of the observed line profiles. Tentative identification is proposed for some of these. Due to possible motions present in the atmosphere surrounding HD 138403, the wavelength of spectral features reported in Table 4 may not correspond any longer to the laboratory wavelength of the unidentified line transition.

4. Conclusions

A description of the far-ultraviolet (1200–2000 Å) spectrum of the low-excitation planetary nebula 315–13°1 has been given in the present paper.

We have stressed the importance of the mass-loss from the central nucleus HD 138403 as revealed by the presence of numerous P Cygni profiles (types I, VIII or IX) for C II, III, IV; N III, IV, V; O IV, V; Si III, IV and He II, giving this object the greatest variety of ions so far observed in the stellar wind of a planetary nebula. Although the terminal velocities are found to be of the order of 800 km s^{-1}, it is not excluded that greater velocities ($\sim$1300 km s^{-1}) are attained by discrete blobs of matter driven away from the central star. In this context and with the known fact that HD 138403 is a rapidly evolving object (see Paper I), it would be imperative to collect additional ultraviolet spectra in order to search for variability in the UV line profiles. Such observations would certainly also shed more light on the nature, role and mechanism of mass-loss present in most – if not all – planetary nebulae (Benvenuti and Perinotto, 1980).

Nussbaumer (1980) has mentioned that for the dynamic range attainable with IUE observations, the ratio between the line fluxes measured for the magnetic quadrupole and dipole transitions of C III] can help in density determinations for $n_e \lesssim 5.5\,10^5$ cm^{-3}. This ratio has been previously measured in IC 4997 (Flower et al., 1979) as 0.06 ($n_e \sim 510^5$ cm^{-3}), in NGC 7027 (Ponz cited in Nussbaumer and Schild, 1979) as 0.6 ($n_e = 510^4$ cm^{-3}), in NGC 6210 and NGC 7009 (Köppen and Wehrse, 1980) as 1.2 and 1.1 ($n_e \sim 10^4$ cm^{-3}). In a similar way and for the case of 315–13°1, we have been able to derive $n_e = 1.1$ (± 0.4) 10^5 cm^{-3} for the electron density in the main nebula. Furthermore, identifying the spectral feature seen in the red wing of the C III] λ 1908.734 emission profile with an emission satellite due to the dipole transition, a lower limit $n_e \gtrsim 3.7\,10^5$ cm^{-3} has been inferred for the electron density prevailing in the receding lobe of a bipolar structure, assumed to be responsible for a similar splitting of the Balmer (H_β–H_9) and [O II] λλ 3726, 3729 emission lines. These UV data also support the hypothesis that this bipolar structure is expanding around HD 138403 with a velocity $v_s \sim 122$ km s^{-1}, via the selective radiative process of edge and/or line locking mechanism(s) (see Paper I).

Acknowledgements. One of us (J. S.) acknowledges financial support from the "Fonds National de la Recherche Scientifique" (Belgium) during the observational phase of this work. We wish also to thank the "Centre de Données Stellaires de Strasbourg", specially Agnès Acker, for providing us with an extensive bibliography of the planetary nebula HD 138403. Our thanks also go to Dr. de Boer for some helpful comments.

References

Abbott, D.C., Bohlin, R.C., Savage, B.D.: 1982 (preprint)
Beals, C.S.: 1951, *Publ. Dominion Astrophys. Obs.* **9**, 1
Benvenuti, P., Perinotto, M.: 1980, Proc. Symp. The Second Year of IUE, ESA SP-157 p. 187
Boggess, A., et al.: 1987a, *Nature* **275**, 372
Boggess, A., et al.: 1978b, *Nature* **275**, 377
Castor, J.I., Lamers, H.J.G.L.M.: 1979, *Astrophys. J. Suppl.* **39**, 481
de Boer, K.S., Nash, A.G.: 1982, *Astrophys. J.* **255**, 447
Fitzpatrick, E.L., Savage, B.D., Sitko, M.L.: 1982, *Astrophys. J.* **256**, 578
Flower, D.R., Nussbaumer, H., Schild, H.: 1979, *Astron. Astrophys.* **72**, L1
Georgelin, Y.M., Georgelin, Y.P., Sivan J.-P.: 1979, IAU *Symp.* **84**, p. 65
Gilra, D.P., Pottasch, S.R., Wesselius, P.R., Van Duinen, R.J.: 1978, *Astron. Astrophys.* **63**, 297
Harvel, C.: 1980, NASA IUE Newsletters **10**, 32
Heap, S.R.: 1977a, *Astrophys. J.* **215**, 609
Heap, S.R.: 1977b, *Astrophys. J.* **215**, 864
Hutchings, J.B.: 1978, *Earth Extraterr. Sci.* **3**, 123
Kelly, R.L., Palumbo, L.: 1973, NRL Dept. No. 7599
Koelbloed, D.: 1962, *Bull. Astron. Inst. Neth.* **16**, 163
Köppen, J., Wehrse, R.: 1980, Proc. Symp. The Second Year of IUE, ESA SP-157, p. 191
Loulergue, M., Nussbaumer, H.: 1976, *Astron. Astrophys.* **51**, 163
Méndez, R.H., Niemela, V.S.: 1979, *Astrophys. J.* **232**, 496
Milne, E.A.: 1926, *Monthly Notices Roy. Astron. Soc.* **86**, 459
Nussbaumer, H., Schild, H.: 1979, *Astron. Astrophys.* **75**, L17
Nussbaumer, H.: 1980, Proc. Symp. The Second Year of IUE, ESA SP-157, p. XLIII
Olson, G.L.: 1978, *Astrophys. J.* **226**, 124
Osterbrock, D.E.: 1970, *Astrophys. J.* **160**, 25
Pottasch, S.R., Wesselius, P.R., Wu, C.C., Fieten, H., Van Duinen, R.J.: 1978, *Astron. Astrophys.* **62**, 95
Savage, B.D., de Boer, K.S.: 1981, *Astrophys. J.* **243**, 460
Snow, T.P., Morton, D.C.: 1976, *Astrophys. J. Suppl.* **32**, 429
Snow, T.P., Jenkins, E.B.: 1977, *Astrophys. J. Suppl.* **33**, 269
Surdej, J.: 1980, *Astrophys. Space Sci.* **73**, 101
Surdej, A., Surdej, J., Swings, J.P.: 1982, *Astron. Astrophys.* **105**, 242 (Paper I)
Thackeray, A.D.: 1950, *Monthly Notices Roy. Astron. Soc.* **110**, 524
Thackeray, A.D.: 1956, *Vistas in Astronomy* **2**, 1380